3 Physics and Technology of Fusion

The activities on the physics of fusion plasmas form a large part of the IPPLM Association programme. They were carried out along three main lines: theory and modelling of tokamaks, plasma-wall interaction and the development of plasma diagnostics. Technology works were devoted to structural materials for low temperature cooling concept, divertor shield materials, joining technology, modelling of structure and properties of iron and iron alloys, nuclear data studies/experiments in support of TBM activities and studies in the field of cooling techniques for HTS fusion windings. Inertial fusion energy (IFE) "keep-in-touch" activity was focused on the analysis of emerging options of IFE on the basis of results of experiments and numerical modelling.

- **Theory and modelling of tokamaks**
  - Support to the advancement of the ITER Physics Basis
    Including:
    - WP13-ITM-ISM-ACT1-01/IPPLM Support to the validation and physics application of the ETS and ITM workflows
    - WP13-ITM-IMP3-ACT1-01/IPPLM Maintenance, continuous development, verification and validation of the ETS and other core components
    - Core Programming Team - full-time support action for ISIP (ITM TF)
    - WP09-HPC-HLST TA Participation to the work of the HLST
    - WP13-ITM-ISIP-ACT3-01/IPPLM Identify and develop missing functionalities in the framework
    - WP13-ITM-ISIP-ACT1-01/IPPLM Support the users of the framework
    - Numerical and analytical study of nonlinear evolution of waves driven by energetic ions in a tokamak plasma close to instability threshold
    - Modelling of the emission spectrum structures for tungsten ions
    - WP13-IPH-A11-P2-01/IPPLM Ways to extend the operational window of high-Z PFCs by external impurity seeding
  - Activities in support to the DEMO design
    Including:
    - Preliminary analysis of the scenario consistency with the edge and divertor constraints, including proper treatment of impurities. Modelling of DEMO reactor with the help of COREDIV code
    - Participation to the EFDA DEMO modelling studies in the field of SYS, PEX and DTM
    - WP13-SYS-01-B-T05-01/IPPLM Impact of DEMO Scenario on design
    - WP13-SYS-02-T10-01/IPPLM Benchmarking of MC tools on DEMO model

- Support to the users of the ITM framework and for fusion modelling
  Including:
  - WP13-PEX-02-T02-01/IPPLM Extend Physics Assessment of Novel Configurations
  - Numerical simulations with the COREDIV code of plasma parameter in the WEST project

- **Plasma-wall interaction**
  - Support to the advancement of the ITER
    Including:
    - WP13-IPH-A01-P1-01/IPPLM Provide experimental input for material migration and mixed material formation in tokamak devices
    - WP13-IPH-A01-P1-02/IPPLM Nitrogen retention and global deposition pattern in ASDEX and TEXTOR
    - WP13-IPH-A01-P3-02/IPPLM Influence of mixed surface layers on fuel retention and release
    - WP13-IPH-A03-P1-02/IPPLM Microscopic investigation of radiation damage in tungsten and its influence on deuterium retention
    - WP13-IPH-A03-P2-01/IPPLM Determination of dust morphology by unified dust analysis methods
    - WP13-IPH-A03-P2-02/IPPLM Assessment of Fuel Removal Methods and Dust Generation
    - WP13-IPH-A11-P3-01/IPPLM High Power ICRH operation with metallic plasma facing components High power ICRF with high Z Wall
  - Activities in support to the DEMO design
    Including:
    - WP13-PEX-03a-T02-01/IPPLM Preparation and characterization of the bulk steel tiles
    - WP13-PEX-03a-T03-01/IPPLM Erosion behaviour of W-containing steels. Laboratory measurements and impurity influx in tokamaks from eroded samples
    - WP13-PEX-03a-T03-02/IPPLM Erosion behaviour of W-containing steels. Laboratory measurements and impurity influx in tokamaks from eroded samples

- **Fusion plasma diagnostics**
  - Development of nonconventional procedure of polarimetric data inversion in conditions of comparable Faraday and Cotton-Mouton effects
  - Feasibility studies of hard X-ray technique for the future HXR monitor
  - WP13-DAS-04-T02-02/IPPLM Review of DEMO Diagnostic Issues and Requirements, R&D plan for CDA
  - WP13-DAS-04-T06-02/IPPLM Neutron, gamma ray and Soft X-ray diagnostics
  - Applications of solid-state nuclear track detectors (SSNTDs) for fast ion and fusion reaction product measurements in tokamak experiments
  - Determination of emission characteristics of fast electron streams within Tore-Supra and other MCF experiments

- CVD diamond detectors for plasma measurements
- Diagnostics for magnetic confinement plasma – COMPASS: neutron and ion measurements and calculations
- Detection of the delayed neutrons from activation of fissionable materials in the neutron field at fusion-plasma devices
- Development of soft X-ray triple GEM gas detector for energy resolved soft x-ray plasma diagnostics
- WP13-IPH-A02-P3-01/IPPLM Development of new MHD diagnostic: GEM gas detector for Soft X-ray measurement
- Development of new hardware and firmware for GEM detector dedicated to neutron and soft x-ray position and energy measurement
- WP13-IPH-A09-P2-01/IPPLM Neutron yield monitor as an indicator of fast particles confinement

- **Emerging technologies**
  - Development of material science and advanced materials for DEMO

    Including:
    - Divertor shield - verification of TiC addition and improving fabrication capacity
    - WP13-MAT-HHFM-01-01/IPPLM/BS Armour materials
  - Materials modelling
    Including:
    - Influence of helium bubble on mechanical properties of iron
    - WP13-MAT-IREMEV-03-01/IPPLM Deformation and plasticity
    - WP13-MAT-IREMEV-05-01/IPPLM Experimental validation of models
    - WP13-MAT-IREMEV-05-02/IPPLM Experimental validation of models
  - Development of HT superconductors for DEMO
    Including:
    - WP13-DAS-01-T03-01/IPPLM Iteration of the conductor analysis for both RW and WR options
    - WP13-DAS-01-T09-01/IPPLM| WP13-DAS-01-T09-02/IPPLM Preparation of the SULTAN facility for testing of high-current HTS conductors at variable temperatures(PS)

- **Inertial fusion energy “keep-in-touch” activity**
  - Analysis of emerging options of IFE on the basis of results of experiments and numerical modelling

3.1 Theory and modelling

Corresponding author **Roman Stankiewicz**
roman.stankiewicz@ifpilm.pl

Introduction

The IPPLM Euratom association activities in theory and modelling include the participation in ITM (Integrating Tokamak Modelling) project in developing the system codes in Kepler platform as well as in support of informatics structures in order to improve the efficiency and extend the possibility of using the developed tools on various computation platforms. The great part of activity is connected with analyses of various existing tokamaks (e.g. JET, ASDEX) and performance of planned future tokamaks and power plants (ITER, DEMO) with special attention devoted to core-edge coupling very important for case of tungsten used as plasma facing component. The new type of divertor (snowflake) has been analysed. The other activities cover the fast ion driven modes, the tungsten spectra in temperature relevant to ITER, Monte Carlo methods in analyses of neutron distribution.

Maintenance, continuing development, verification and validation of the ETS and other core components. Participation in ITM project (Integrated Tokamak Modelling).

The procedure has been developed to use core transport codes (CRONOS ,JETTO, ASTRA) in the core and take into account the coupling between core and scrape off layer and sputtering of tungsten at target plates with help of COREDIV code. Transport codes and COREDIV are used iteratively. Transport codes provides the magnetic equilibrium, the current diffusion, the auxiliary heating and current drive and transport simulations for main ion species inside the sepatarix while the COREDIV code completes these simulations with impurity distribution and radiation, taking into account the core-SOL-divertor coupling.

The ETS (European Transport Simulator) was applied to simulate impurity transport for the conditions of JET discharge #82794 (ITER-like wall) under the condition: profile of the electron density are prescribed, for bulk ions Bohm-Gyro-Bohm diffusion plus extra diffusion coefficient and pinch velocity for impurity are used, the density of impurities (W, Be, Ni) at the separatrix with coronal distribution on ionization stages are adopted to have Zeff and total radiation in agreement with experimental data. Good agreement between experimental and calculated profiles of radiation has been achieved.

The Kepler workflow has been prepared for testing the stabilisation of ETS for stiff transport problem.

Informatics supports necessary to accomplish the final goal of ITM project.

The PSNC activity in 2013 (referring to EFDA ITM-TF 2013 Workprogramme and to the EFDA-HLST) included the following tasks:

- **Core Programming Team** - full-time support action for ISIP (ITM TF)
- **WP09-HPC-HLST TA** - Participation to the work of the HLST
- Identify missing functionalities in the platform and develop the required new functionalities (**WP13-ITM-ISIP-ACT3-T01**): Deploy strategies for HPC and GRID execution of components and workflows. It includes the deployment of the procedures and tools prepared in past years for executing components of advanced physics workflows on HPC and GRID facilities. It includes also the evaluation of the proposed strategies and the design of new ones when needed depending on the Use Case. The task includes also the maintenance of GRID and HPC services on the Gateway and the consistent evolution of HPC2K.
- Support the users of the ITM platform (**WP13-ITM-ISIP-ACT1-T02**): provision of tutorials on ITM tools and Kepler during ITM general meeting and code camps

Nonlinear dynamics of fast ion driven plasma modes near instability threshold – theoretical basis for integrated tokamak modelling

The population of fast particles in a tokamak plasma could destabilize wave modes due to wave-particle interaction and have important influence on the energy distribution and transport phenomena. Theoretical investigations of the dynamics of the wave modes, especially the nonlinear stages of the dynamics, have been analyzed The Fermi like model has been generalized for the case with weak magnetic fields and implemented in C++ code. The algorithm of the model has been generalized to describe a two-mode plasma wave case.

Modeling of the emission spectrum structures for tungsten ions

Investigations concerning the influence of outer-shell electron stripping on the positions of various K, L and M x-ray lines for tungsten, obtained using the multi-configuration Dirac-Fock method have been done. Moreover, the modeling of the L and M x-ray line structures for tungsten in high temperature plasmas predicted with temperatures relevant to large tokamaks including the JET and the future ITER has been performed using the Flexible Atomic Code within the framework of the collisional–radiative (CR) model. For L x-ray lines, the results predicted for various levels of CR model sophistication have been compared with the spectrum measured using the electron beam ion trap (EBIT) calorimeter spectrometer at the Livermore SuperEBIT that constitutes a rigorous atomic benchmark for tokamak plasmas. In the case of M x-ray lines, the experimental SuperEBIT spectra as a superposition of theoretical contributions for different ions has been reproduced. The results of the simulations could be used to reliable interpretation of forthcoming spectra registered using the high-resolution x-ray crystal spectrometer (KX1) on JET and can be used with confidence to define the capabilities needed for ITER's high-resolution x-ray diagnostic.

Ways to extend the operational window of high-Z PFCs by external impurity seeding

Fusion performance of ITER H-mode plasmas in the presence of intrinsic (He, Be and W) and seeded (Ne) impurities has been investigated in self-consistent core-pedestal-SOL simulations for two values of pedestal density $n^{ped}_e = 6.12 \times 10^{19} m^{-3}$ (reference case) and $n^{ped}_e = 9.0 \times 10^{19} m^{-3}$ using the COREDIV and JETTO codes. The theory-based GLF23 transport model which predicts a relatively high density peaking ($n_{e0}/\langle n_e \rangle = 1.37 \div 1.39$) has been used for this study. For medium density case the H-mode operation with a power across the separatrix well above the L-H power threshold has been obtained, but the divertor heat loads exceed $10 MW/m^2$. Neon gas puff strongly reduces the power to divertor plate in this scenario, increasing at the same time the tungsten sputtering by Ne that leads to even larger core radiation and dilution, than in the case without Ne. As a result, the medium density H-mode operation with Ne seeding and low divertor heat loads is barely above the L-H power threshold. This operational point is weakly sensitive to tungsten inward pinch due to a strong coupling between W transport, radiation and sputtering. At high density with much larger core radiation ($90 MW$), the possibility of H-mode operation strongly depends on the choice transport model, with the power through the separatrix well below the L-H power threshold in simulations with the GLF23 and above for ($H98y$ scaling-based) transport model.

Numerical analyses of base line DEMO design concepts with the COREDIV code

The new DEMO design concepts, obtained by system code PROCESS has been analysed numerically with the help of COREDIV code describing self-consistently the core and the scrape of layer (SOL) with divertor region. The consistency of the plasma parameters has been checked. The obtained global parameters using COREDIV are close to those proposed by PROCESS but depend strongly on seeded impurities concentration and velocity pinch. The possibility of reduction of the power load to divertor plate using seeded impurities has been investigated. The dependence of plasma parameters on pinch velocity and additional heating power has been analysed.

It has been found, that usually there is a limit on admissible concentration of impurities above which the self-consistent COREDIV solution does not exist. This limit is defined by dilution of plasma (helium) and

impurity radiation. However, in some separated cases, detached like solutions exist for which the power to plate is reduced to zero. In this cases the sputtered impurity concentration (W) is equal to zero and the seeded impurities can radiate in the SOL the total power flowing from the core region. Further works are planned to analyse this kind of solutions in detail.

Benchmarking of MC tools on DEMO Monte-Carlo simulations of neutron distribution at DEMO

A work on Monte Carlo simulations of neutron distributions at DEMO was continued. The IPPLM contribution to task WP13-SYS-02-T10-01 is described in this report. The attempts have been made to convert geometry of DEMO from CAD to MCNP and FLUKA. Possibility of writing a special neutron source subroutine for FLUKA has been analysed. Possible future activities are proposed.

TECXY code simulation of the snowflake divertor configuration in DEMO reactor

Comparison between the snow flake SF and the conventional divertor SN has been carried out with the 2D edge code TECXY in the case of the DEMO project. The code takes into account all the plasma physics effects occurring in the scrape off layer but simplifies the overall neutral dynamics, considering a simple geometry for the divertor plates and an analytical model for the neutrals recycling.

The SF divertor performs up to 2.5 times better than SN as far as heat flux density mitigation is concerned. The plasma cooling in case of snowflake divertor is particularly advantageous over the SN case for DEMO-relevant separatrix densities. The effect cannot be ascribed to favorable geometry (on the contrary, $f_{q,\,\mathrm{geom}}<1$), and is likely caused by increased divertor-region neutral radiation. The SF configuration picked is still not optimal and needs improving, but the simulation results are already promising. The code is ready to scan parameter space for both non-seeded and seeded discharges.

Numerical simulations with the COREDIV code of plasma parameters in the WEST tokamak

The COREDIV model has been applied to study core-edge coupling mediated by tungsten for WEST. For all configurations, an acceptable level of tungsten is found with low radiation levels. Simultaneously, tolerable heat loads to the plate are observed, at ITER relevant levels. The power to the plate saturates when heating increases (for a given density). Changes to average or separatrix density can strongly influence the results. Self-sputtering appears to be the dominant mechanism for tungsten production. This effect of core-edge coupling increases strongly with light impurities (here boron), because the sputtering threshold for boron on tungsten is much lower than for deuterium. The influence of light impurities on the plasma behaviour has been analysed.

Collaboration

Association EURATOM – CEA, Cadarache, France
Association EURATOM – CCFE, Culham, United Kingdom
Association EURATOM – ENEA, Frascati, Italy
Association EURATOM – IST, Lisbon, Portugal
Association EURATOM – Belgian State, Brussels, Belgium

3.2 Plasma-Wall Interaction

Corresponding author **Elżbieta Fortuna-Zaleśna**
efortuna@inmat.pw.edu.pl

Introduction

The work carried out in the framework of the Plasma-Wall Interaction block includes activities from the following EFDA tasks:

1. WP13-IPH-A01-P1-01/IPPLM Provide experimental input for material migration and mixed material formation in tokamak devices
2. WP13-IPH-A01-P1-02/IPPLM Nitrogen retention and global deposition pattern in ASDEX and TEXTOR
3. WP13-IPH-A01-P3-02/IPPLM Influence of mixed surface layers on fuel retention and release
4. WP13-IPH-A03-P1-02/IPPLM Microscopic investigation of radiation damage in tungsten and its influence on deuterium retention
5. WP13-IPH-A03-P2-01/IPPLM Determination of dust morphology by unified dust analysis methods
6. WP13-IPH-A03-P2-02/IPPLM Assessment of Fuel Removal Methods and Dust Generation
7. WP13-IPH-A11-P3-01/IPPLM High Power ICRH operation with metallic plasma facing components
8. WP13-PEX-03a-T02-01/IPPLM Preparation and characterization of the bulk steel tiles
9. WP13-PEX-03a-T03-02/IPPLM Erosion behaviour of W-containing steels. Laboratory measurements and impurity influx in tokamaks from eroded samples
10. WP13-PEX-03a-T03-01/IPPLM Erosion behaviour of W-containing steels. Laboratory measurements and impurity influx in tokamaks from eroded samples

The activities in the above listed tasks were undertaken as a support to the advancement of the ITER Physics Basis and DEMO design.

Results

1. The investigations of a sample from a bulk tungsten tile (from Brg. 1) exposed at the outer strike point during the 2010/2011 campaign in ASDEX Upgrade were carried out. The aim of these post-mortem analyses (SEM, FIB, TEM) was to describe materials mixing and plasma-induced damage, with special attention to crack formation and recrystallisation. Observations of the sample revealed three cracks which start at the tile channels. One crack starts at the channel present at the tile side and penetrates to the tile surface. Two of them extend between the channel present at the tile bottom and the channel at the tile side. The observation at the cross-sections revealed near to the tile surface a 3µm thick zone of sub-micron grains. At the surface 150-700 nm deposit is present. It contains tungsten, carbon and boron.

2. Nitrogen is foreseen as seeding species. Samples of tungsten and graphite from N-15 and WF6 tracer experiments from TEXTOR have been studied. The investigations included characterization of the surface morphology by HRSEM and examinations of their chemical composition by EDS and XPS techniques. The maximum level of nitrogen detected by XPS technique amounted to 6 at.%. TEM examinations of the surface layer of the samples revealed presence of tungsten carbides.

3. Investigation of the behaviour of the surface of plasma facing materials (mixed materials) samples, bulk tungsten and stainless steel samples after interaction with laser pulses and plasma and ion streams in terms of fuel retention and release were carried out. As the source of heat-loads the pulsed ns-laser systems and plasma accelerator of the PF type capable of ensuring the surface heat load at level from 0.5 to 5 MJ/m^2 were used. The experiments were oriented for the following goals (i): comparison of the deuterium contents (by the LIBS – Laser Induced Breakdown Spectroscopy) in mixed material and bulk

samples, (ii) observation of the aging effects on the retention in the mixed material layers and (iii) demonstration of the application of the DP-LIBS (Dual Pulse LIBS) method for WAlC layers.

4. TEM investigations of neutron-like damage in two tungsten samples simulated by 20 MeV W^{6+} implantation at room temperature were performed (fluencies of $3.7*10^{18}$ and $1*10^{19}$ W/m^2). The radiation damage structure has been analysed in post-irradiation state as well as after annealing at 673 K, 773 K, 950 K and 1000 K for 1h. The annealing was performed in order to monitor the irradiation damage recovery. The STEM observations showed that the depth of damaged zone differed and is equal to 2.5 µm and 2.8 µm for $3.7*10^{18}$ and $1*10^{19}$ W/m^2 doses, respectively. It has been also observed that the depth of damage volume was influenced either by the crystallographic orientation of the target or the presence of grain boundary in the ion beam affected target volume. The damaged zone can be divided into 3 sub-regions: (1) near surface area with high density of dislocations, (2) intermediate area with lower density of "long" dislocations and (3) deep region with high density of "short" dislocations. Annealing of the W lamellae leads to aggregation of small defects and rearrangement as well as partial healing of dislocations. At the temperatures applied only the irradiation-induced damage underwent this recovery, while structural dislocations remained intact even at the highest annealing temperature of 1000K.

5. The examinations on dust particles trapped in the membrane rims of filters no 1 and 8, collected after 2009 ASDEX Upgrade campaign were carried out. Filter no 1 represents the dust at the low field side midplane and filter 8 the outer divertor structure. The dust particles have been investigated in terms of their size/morphology, composition and structure by scanning electron microscopy (SEM) combined with energy-dispersive X-ray spectroscopy (EDS), focused ion beam (FIB) and transmission electron microscopy (TEM). The aim of the investigations was to obtain information on the origin of dust particles and to broaden the knowledge about relevant processes of dust formation and mobility. The tungsten based particles were of special interest. They can be categorised into three classes: spherical, irregular and flakes, each about 1/3 of the total population. Spherical tungsten dust particles found in our examinations are interpreted as droplets released during arcing. Concerning the tungsten particles rich in boron, their morphology is the same as the deposited layers at the inner divertor baffle region, close to the arcs tracks (fractionised/destroyed by arcing).

6. Experiments of laser-removal of deuterium containing mixed material layers of tungsten, aluminum and carbon from tungsten substrate have been performed both in air and in a vacuum chamber. As a source for removal a Nd:YAG laser with fluences about 2, 14 and 25 J/cm^2 was used. The LIBS (Laser induced Breakdown Spectroscopy) method was applied for investigation of laser pulse-sample interaction. By means of LIBS it was possible to observe that for 25 J/cm^2 the mixed materials W:Al:C layer of about 3 µm thickness has been removed after 7 laser shots. For lower energy densities the W:Al:C layer has not been removed even after 10 laser shots while for deuterium, there were no difference observed depending on applied fluences and in all cases this layer was removed after 1-2 laser pulses. The research was focused on investigation of the effects of the laser irradiation on morphology and microstructure of deposits and substrates. The morphology of the sample before and after laser irradiation was characterized by scanning electron microscopy, scanning transmission electron microscopy, focus ion beam and energy-dispersive X-ray spectroscopy.

7. Experimental data from full tungsten (W) ASDEX Upgrade (AUG) machine allowed characterization of the processes participating in the ICRH (Ion Cyclotron Resonance Heating) specific plasma wall interaction, which can help to maximize ICRH power in ITER. Long-term observation of W concentration in H-mode deuterium plasmas produced in AUG tokamak was completed by calculation of the tungsten concentration for the discharges with ICRH in use in experiments carried out in 2013. Tungsten was diagnosed by passive spectroscopy in the vacuum ultraviolet (VUV) range. Analysis were performed based on the spectroscopic observations of W quasi-continuum (around λ= 5 nm) and lines radiation. In addition, for all analyzed discharges, effective tungsten yield (Yeff), defined by ratio of tungsten and deuterium influxes measured at the antenna limiters has been evaluated. Tungsten influx was monitored by measuring WI line radiation at 400.8 nm. To calculate the deuterium influx, the Balmer-d transition at 410.1 nm was used. Moreover, the effect of injection of different gases on W release during ICRH has

been investigated. The stress was put mainly on injections of deuterium (D_2) and deuterium with nitrogen (N_2), argon (Ar) and krypton (Kr). In the analysis, discharges for H-mode deuterium plasma with the plasma current Ip = 1 MA, have been considered. In such condition most of the pulses were only with the antenna a1 and a2 powered. The conducted research allows to state that operation of ICRH antennas in magnetic fusion experiments is often accompanied by enhanced plasma-surface interactions. Long-term spectroscopic observations indicated slow shot-to-shot reduction of the core W concentration and Yeff in the AUG plasma during ICRH operation. The effect of gas injection seems to have beneficial effect on the ICRH plasma performance. The W concentration decreased strongly with increasing of gas puff regardless of the type of injected gases. Higher level of W content was found in ICRH than in NBI heated discharges.

8/9. The present studies were carried out on samples received from IPP Garching for microstructural investigations:

1. EUROFER sample, mechanically polished for laboratory experiments (Very flat surface. TEM examinations revealed: large carbides 70-400nm, located mainly at grain/subgrain boundaries and small ones 10-15nm, located inside grains, often arranged/aligned in chains. Precipitations are complex Fe-Cr-W-Co carbides).
2. P92 sample after wire erosion cutting (Surface re-melted. Residue of wire material present. Material mixing, cracks and delaminations in the sub-surface region).
3. P92 sample after glass pebble blasting (Surface flaking. Small fragments of pebbles embedded into surface. Crack and delaminations in the sub-surface region).
4. P92 sample after electropolishing. (Flat surface. TEM examinations revealed complex Fe-Cr-W carbides of the size 80-400nm, located mainly at subgrain/lath boundaries).

EUROFER was the same sample type used in erosion experiments in the Garching High Current Ion source. The P92 steel samples were the same material and production method for the two rows of bulk steel tiles, which were installed in ASDEX Upgrade during the last shutdown.

10. The laser interaction with stainless steel samples with tungsten layers deposited by laser at IPPLM were examined. As a source a Nd:YAG laser with energy of 200mJ at 1st harmonic, in a 10ns pulse was used. The LIBS (Laser Induced Breakdown Spectroscopy) method was applied for investigation of laser pulse-sample interaction. The morphology of the sample before and after laser irradiation was characterized by scanning electron microscopy, focus ion beam and energy-dispersive X-ray spectroscopy.

Conclusions

Observations of the sample from a bulk tungsten tile (from Brg. 1) exposed at the outer strike point during the 2010/2011 campaign in ASDEX Upgrade revealed three cracks which start at the tile channels. One crack starts at the channel present at the tile side and penetrates to the tile surface. Two of them extend between the channel present at the tile bottom and the channel at the tile side.

The irradiation damage recovery was examined on tungsten implanted with 20 MeV W^{6+}. The STEM observations revealed that annealing of the W lamellae leads to aggregation of small defects and rearrangement as well as partial healing of dislocations. At the temperatures applied (673-1000K) only the irradiation-induced damage underwent this recovery, while structural dislocations remained intact even at the highest annealing temperature of 1000K.

There is a large diversity in morphologies and internal structures of tungsten-based particles which are the largest group of dust particles in AUG. The analyses carried out at the particles containing tungsten, boron and carbon prove that the intermetallic phases both carbides and borides are present in the dust particles/deposited layers.

The preliminary research showed that standard q-switched Nd:YAG laser pulses (i.e. with an energy of a part of J and time duration of a few ns) can be used for fuel removal from the first wall together with the mixed materials layer (co-deposited layer).

The conducted research on full tungsten (W) ASDEX Upgrade (AUG) machine allows to state that operation of ICRH antennas in magnetic fusion experiments is often accompanied by enhanced plasma-surface interactions. Long term spectroscopic observations indicated slow shot-to-shot reduction of the core W concentration and Y_{eff} in the AUG plasma during ICRH operation. The effect of gas injection seems to have beneficial effect on the ICRH plasma performance. The W concentration decreased strongly with increasing of gas puff regardless of the type of injected gases. Higher level of W content was found in ICRH than in NBI heated discharges.

Collaboration

Association EURATOM – VR, Stockholm, Sweden,
Association EURATOM – IPP, Garching, Germany
Association EURATOM – FZJ, Jülich, Germany
Association EURATOM – IPP.CR, Prague, Czech Republic
Association EURATOM – ENEA, Frascati, Italy

References

[1] O.V. Ogorodnikova, K. Sugiyama, Ł. Ciupiński, J. Grzonka, Yu. Gasparyan, V. Efimov, Annealing of radiation-induced damage in tungsten under and after irradiation with 20 MeV self-ions, submitted to Journal of Nuclear Materials.
[2] Ł. Ciupiński et al., TEM Observations of Radiation Damage in Tungsten Irradiated by 20 MeV W ions, Nuclear Inst. and Methods in Physics Research, B (2013), pp. 159-164
[3] E. Fortuna-Zaleśna, J. Grzonka, M. Rasiński, M. Balden, V. Rohde, K.J. Kurzydłowski, ASDEX Upgrade Team: „Characterization of dust collected after plasma operation of all tungsten ASDEX Upgrade", Physica Scripta article in press
[4] P. Gąsior, et al., Journal of Nuclear Materials 390–391 (2009) 585–588
[5] D. Ivanova, et al. Physica Scripta, T145 (2011) 014006
[6] M. Kubkowska, et al., Journal of Nuclear Materials 438 (2013) S750–S753

3.3 Fusion plasma diagnostics

Corresponding author **Monika Kubkowska**
monika.kubkowska@ipplm.pl

Introduction

The work conducted in the framework of the plasma diagnostics in 2013 included activities in the following areas:

- Method of polarimetric data inversion;
- Feasibility studies of hard X-ray technique for the future HXR monitor
- Review of DEMO diagnostics issues and requirements
- Investigation of different detectors for plasma measurements - Cherenkov, CVD diamond and solid-state nuclear track detectors (SSNTDs);
- Neutron and ion measurements and calculations on the COMPASS tokamak
- Detection of the delayed neutrons from activation of fissionable materials in the neutron field at fusion-plasma devices
- Development of soft X-ray triple GEM gas detector with new hardware and firmware for energy resolved soft X-ray plasma diagnostics
- Neutron yield monitor as an indicator of fast particle confinement

Presented work in many cases describes a continuation of investigations done by IPPLM-Association group in the previous year.

Diagnostics used in thermonuclear reactor DEMO will be exposed to extremely hard working conditions. There will be very high fluxes of neutrons and gamma radiation. Many technical problems have already been solved or will be solved during the development of diagnostics for ITER. Unfortunately, a lot of those systems will not be adequate for DEMO. It is necessary to review the current status of technology and R&D in each of the relevant segments. The development of novel techniques to be applied in DEMO and following commercial thermonuclear power plants has to be considered. Particular emphasis should be placed on the development of systems detecting emission of neutrons from thermonuclear reactions because it will be an essential component for monitoring in DEMO.

What is more, a high-resolution X-ray spectroscopy is a powerful tool for diagnostics of plasma state evolution in a tokamak. X-ray spectra in tokamak plasma origin from continuum (bremsstrahlung) and characteristic atomic radiation which provides accurate information on the crucial plasma parameters such as impurity concentration, ion temperature, and the toroidal rotation velocity. At JET two independent diagnostic channels, based on the Bragg crystal X-ray spectroscopy (with very high energy resolution, E/ΔE up to 20 000, comparable to the natural widths of the measured X-ray lines allowing very good selectivity), have been set for monitoring plasma emission spectra at specific photon energy windows what corresponds to specific diffraction orders.

Nowadays, there is a growing interest in developing a reliable method for the measurement of the internal magnetic field in high temperature, magnetically confined plasmas. A special need for such diagnostic arises in the investigation of the tokamak devices in which the measurement of the poloidal field distribution would yield the plasma current density profile. Additionally, the appearance and growth of numerous instabilities are closely connected to the existence of certain rational surfaces in the plasma as well as subtle local modifications of the poloidal magnetic field. Information of all these parameters are essential for understanding confinement, stability and energy balance of the tokamak plasma.

Also, an investigation of hard X- and gamma-ray diagnostics of tokamak plasmas is needed. In 2013 the CsI:Tl, NaI:Tl, LaBr3:Ce, CeBr3 and GAGG:Ce scintillators were investigated. The light output, energy resolution, non-proportionality of the response, decay time and full energy peak efficiency were

measured. Taking into account specific requirements for gamma-ray measurements in fusion devices (operation in a harsh radiation environment, high count rate, high energy resolution and detection efficiency for MeV gamma-rays), the LaBr3:Ce and CeBr3 scintillators are proposed as best candidates for this purpose.

Results

In 2013, the proposed method of polarimetric data inversion has been studied in two areas: extension of theoretical background of the method to the case of multiparameter plasma models and rewriting the numerical code to the occasion of strong coupling between Faraday and Cotton-Mouton effect, when differential equations describing polarization state evolution combine nonlinearly. Preliminary results of the numerical calculations revealed that the applied method of solving a system of differential equations and the gradient method used for minimizing the error function ensure good convergence under conditions typical for tokamak plasma.

The analysis of scintillation materials for tokamak plasma diagnostics showed that the fastest response is observed for LaBr3:Ce and CeBr3 scintillators. This fact promotes both materials as good candidates for high flux measurements in big tokamaks, especially in D-T experiments. The response of GAGG:Ce and NaI:Tl is one order of magnitude slower, however the decay time is still moderate. A long decay time for the CsI:Tl makes this crystal less useful for tokamak plasma diagnostics, where high fluxes of X- and γ-rays are expected and large amount of pile-ups could occur. The GAGG:Ce sample has the highest detection efficiency from all tested scintillator crystals. At the highest measured energy equal to 1408 keV, the GAGG:Ce is almost one order of magnitude more efficient than NaI:Tl and about five times more efficient than LaBr3:Ce and CeBr3 scintillators of the same size. This is due to the higher density of GAGG:Ce in comparison with other tested materials.

The most important for the operation of thermonuclear reactor based on tokamak would be diagnostics of the magnetic field and neutron monitors. Hall-effect devices will probably be used for measurements of magnetic field. Their usefulness has been already proved, but in order to make them more resistive to neutron radiation and more reliable, development work is carried out. The problem of transmission of low current signals in the vicinity of strong magnetic field has not been solved yet. Concerning fission chambers working as neutron monitors this problem is even more serious. It might be necessary to develop another neutron monitors capable of measurements of neutron flux densities in a range of six orders of magnitude. It is also important, due to the same problem, to install neutron activation measurement systems supported by neutron transport calculations. The spectroscopy of neutron radiation is discussed. Due to the obvious difficulties in deducting the plasma temperature from the neutron energy spectrum, the application of visible and/or soft X-ray radiation spectroscopy is also considered.

In frame of the area of investigation of detectors for plasma parameters measurements a single crystal diamond detectors obtained with the Chemical Vapour Deposition method (scCVD) were tested in view of their possibilities to detect escaping alpha particles (from deuterium-tritium plasma) and other fast ions (from deuterium plasma). A very good usability of thin (50 μm) diamond detectors for spectrometric measurements of alpha particles and other ions was stated and a routine energy calibration method was elaborated. Thick (500 μm) scCVD detectors were tested for 14 MeV neutron detection. The main result of the performed experiments was that a 50 μm scCVD diamond detector, placed in a tokamak vessel and destined to measure energy spectra of the escaping alpha particles, will be insensitive to the accompanying D-T neutron radiation. Monte Carlo modelling of radiation distributions in the measuring vacuum chamber was undertaken in order to support the interpretation of the energy spectra of obtained from the scCVD diamond detectors. The MCNPX code was used with preparation of the input data with SIMRA and MATLAB.

In 2013, the energy resolution of the CR-39/PM-355 detector irradiated with protons and deuterons was investigated. To this end some rectangular samples (~ 1 x 3) with a thickness of 0.5 mm were irradiated with mono-energetic ions of different energies provided by various particle accelerators, but mainly by the “LECH” accelerator (Van de Graaff type).

A runaway electron measurements within Tore-Supra, as performed by means of the calibrated detector, and physical interpretation of obtained results were reported. Continuation of measurements of suprathermal electron beams in COMPASS by means of single-channel Cherenkov detector has been performed. Additional measurements of fast electrons in ISTTOK by means of two-channel Cherenkov measuring head equipped with diamond radiators have been presented. The manufacturing and installation of a prototype Cherenkov detector in FTU facility and preliminary measurements of fast electron beams in 2013 have been done.

In 2013, experiments at COMPASS tokamak were performed to check usability of He-3 detectors as neutron counters and compare signals from the He-3 detectors with available data from associated diagnostics. The analysis was based on the most relevant parameters like the line average plasma density, the plasma current and relevant diagnostics for neutrons and HXRs detection. The average of total number of events collected by He-3 detector in each shot was ~ 103n/shot. However, neutrons reached the detectors thermalized and scattered. The bubble detectors were used in the experiment to verify results from the He-3 counters. The bubble detector provided an instant visible detection and measured neutron dose, independently on the dose rate and thoroughly insensitive to gamma radiation. Detectors were situated near the He-3 counters used as a neutrons monitors on COMPASS. Numbers of counts were relatively high comparing with number of bubbles in BDs after each 10 shots. The most probable scenario for neutron production was a target beam interaction and some of them were coming from runaway electron interactions.

The classic neutron activation method to estimate fusion-neutron flux can be supplemented by a neutron diagnostics method based on detection of the delayed neutrons from activation of fissionable materials in the primary neutron field created by fusion-plasma. The method is based on consideration of a theoretical approach, on interpretation of the relevant experiment, on the detection efficiency of the measuring device, and on a support of the Monte Carlo modelling. In 2013 an influence of using 6 or 8 groups of the delayed neutron precursors in the theoretical description has been considered. Examples for ^{238}U and ^{232}Th have been shown.

In 2013, two triple-GEM detectors with 206x92 mm^2 detection area and 256 channels each were developed and constructed for high-resolution X-ray measurements of spectra originating from the mid- and high-Z impurities in tokamak plasmas. These detectors have been installed at KX1 diagnostic at JET. The electronics using the modern standards of signal processing and signal transmission based on the firmware configured FPGA technique allows an online measurement of energies and impact position of individual photons at high fluxes. Two detecting units provide energy resolved fast dynamic plasma radiation imaging in the SXR with 100 Hz frequency corresponding to 10 ms time of periodic exposures. Detectors were dedicated and optimized for continuous monitoring of plasma radiation emitted by highly ionized metal impurities present at JET tokamak, W^{46+} (at ~2.4 keV) and Ni^{26+} (at ~7.8 keV) with good energy and position resolution.

The prototype GEM detector for the 14 MeV-neutron monitor consists of 12 µm Mylar window with about 0.2 µm aluminium layer on the inner surface, cascade of 3 GEM foils and readout plane with 0.8 mm strip pitch has been developed. Its capability for measuring β-particles was feasible due to selected activation reactions. Suitable Monte Carlo calculations of charged particles transport inside the detector have been performed by MCNP code. Tests, with the prototype GEM detector provided with 6 analogue electronic boards of 96 channels in total, with the β source have been performed.

Conclusions

Presented reports mainly relate to research which is continued from previous years.

The neutron and magnetic field diagnostics are certainly essential to assure reliable DEMO operation. The soft X-ray spectroscopy is considered as one of the most essential diagnostic for DEMO as well. Further investigations still need to be carried out systematically. Elaboration of the mathematical methods to restore the plasma parameters based on limited number of diagnostics is also crucial.

The described experiment carried out at the COMPASS tokamak was introductory for measuring neutrons created in the D-D reaction. Analyses of results did not show clear source of neutron production during Ohmic discharges. However, the collected results confirmed suitability of He-3 detectors for neutrons measurements. The rate of neutron from the D-D reaction was low due to a low temperature, below 1 keV.

To detect the fast electrons the T-GEM gaseous detector with 1D strip readout was constructed. Detection of fast electrons (β particles) by means of the detector has been proved. The obtained result for β-source was a typical spectrum corresponding to so-called minimum ionizing particles, i.e. in this case, the electrons close to the relativistic energies. In spite of that, the obtained spectrum did not restore exactly results of the performed simulations. Therefore, before the test with the neutron source further investigations are needed.

In the presented reports capabilities of Triple-GEM detecting units developed and constructed to fulfil the requirements for soft X-ray monitoring in the JET tokamak have been presented. For this purpose a new hardware and firmware have been developed.

In the framework of Plasma Diagnostics a method of interpretation of energy spectra of ions and neutrons recorded with use of the diamond scCVD detectors was also developed. It is mainly based on the comparison of responses obtained from thin (50 µm) and thick (500 µm) detectors. Distributions of ions in the measuring chamber at the neutron generator were modelled with the Monte Carlo method. The results allow to make tests of the scCVD detectors at tokamak, e.g. COMPASS.

A special ion pinhole camera was designed and constructed at the NCBJ for COMPASS tokamak. This camera will be equipped in SSND of the PM-355 type and will be used to measure fast primary ions and charged fusion reaction products emitted from tokamak plasma.

Some calculations of proton and other ion trajectories have been performed using the Gourdon code to support the planned experiments.

The PM-355 will be precisely calibrated before using in the COMPASS experiments using mono-energetic ions provided by a particle accelerator.

Collaboration

Association EURATOM – UKAEA, Culham, United Kingdom
Association EURATOM – ENEA, Frascati, Italy
Association EURATOM – CEA, Cadarache, France
Association EURATOM – IPP.CR, Prague, Czech Republic
Association EURATOM – IPP, Garching, Germany
Association EURATOM – Belgian State, Brussels, Belgium

References

[1] J. Chrzanowski, Yu.A. Kravtsov, D. Mazon, Nukleonika, 2012, 57(1), 37−41
[2] E. Costley, Towards Diagnostics for a Fusion Reactor, IEEE Trans. Plasm. Sci., Vol 38 No 10, 2010
[3] J. Iwanowska, et al., Nucl. Instrum. Meth. A712, 34-40 (2013)
[4] K. Jakubowska, et al., Proc. 38th European Physical Society Conference on Plasma Physics, P2.036 (2011)
[5] W.M. Zabołotny, et al, Proc. SPIE 8008, 80080F (2011)
[6] K. Poźniak, International Journal of Electronics and Telecommunications, 56 (4), 489-502 (2010)
[7] H. Noulty, et al, Bubble detectors – a maturing technology, Radiat. Meas. 27 (1997), p.1-11.
[8] S. Atzeni., The Physics of Inertial Fusion: Beam Plasma Interaction, Hydrodynamics, Hot Dense Matter,. Clarendon Press (2004), p. 18-20.
[9] A. Szydłowski, A. Malinowska, et al., Radiation Measurements (2013) Vol. 50, 258–260.
[10] K. Malinowska, A. Szydłowski, et al. Review of Scientific Instruments (2013) Vol. 84 No 7, 07351.
[11] L. Jakubowski, M.J. Sadowski, J. Żebrowski, et al., Rev. Sci. Instrum. Vol. 84 (2013) 016107
[12] L. Jakubowski, V.V. Plyusnin, K. Malinowski, et al., Contrib. Plasma Phys. Vol. 53 (2013) 615-622.

3.4 Emerging technologies

Corresponding author **Łukasz Ciupiński**
lukas@inmat.pw.edu.pl

Introduction

The IPPLM Association activities in the thematic area Emerging Technologies were implemented through three sub-projects namely:

a. Development of material science and advanced materials for DEMO
b. Materials modelling
c. Development of HT superconductors for DEMO.

The tasks within those sub-projects were implemented by three universities – members of the Association Research Unit, that is Warsaw University of Technology, AGH University of Technology and West Pomeranian University of Technology. The implemented tasks were devoted to structural material for low temperature cooling concept, divertor shield materials, joining technology for W-SiC structural joints, modelling of structure and properties of iron and iron alloys, nuclear data studies/experiments in support of TBM activities and studies in the field of cooling techniques for HTS fusion windings.

Results

The computed total mass flow rate [1] in shorter conductors of each double layer is presented in Fig. 1. In DL1 the total mass flow rate in CRPP conductor is over 5 times larger than in the ENEA conductor, whereas in DLs 2-9 the total mass flow rate in the CRPP conductors is 1.3 to 1.5 times larger than in the respective ENEA conductors. The total mass flow rate in the coil is assessed to be 224 g/s and 124 g/s for the CRPP and ENEA design, respectively.

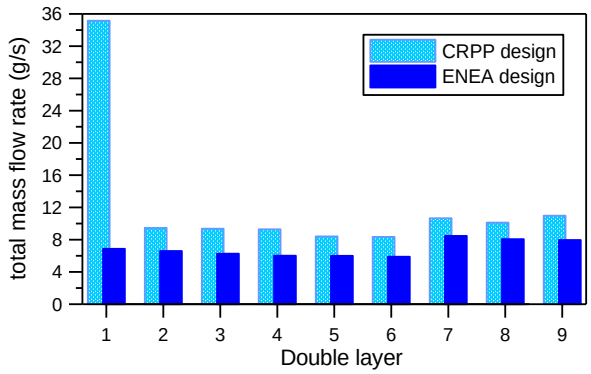

Figure 1. Comparison of the total mass flow rates in the shorter conductor in each DL of CRPP and ENEA coil (no heat deposition).

The assumed heat deposition in the DL1 due to the nuclear radiation is about 100 W. Based on the values of the helium outlet temperature in the 1st conductor in the DL1 calculated for the heat deposition rate equal to 100 W (the most pessimistic scenario – all power deposited in a single conductor) and 50 W (heat deposited evenly in both conductors in DL1) it can be noted that in CRPP conductors the temperature margin is sufficiently large (i.e. larger than 1.5 K) even at 100 W heat deposition, whereas in ENEA conductors the temperature margin is too small even at the heat deposition of 50 W.

The values of the hot spot temperature were calculated for CRPP and ENEA conductors and it was found that both CRPP and ENEA conductor designs fulfil the 150 K hot spot temperature criterion specified in the ITER DDD.

Studying the preparation of the SULTAN facility for testing of high-current HTS conductors at variable temperatures it was assumed that the simplest realisation of HEX would be the coaxial “tube in tube” counter-flow heat exchanger. The thermal – hydraulic analysis of the cryogenic circuit was performed for the inner tube made of copper (RRR = 100) or stainless steel with diameters: D1 = 5 or 6 mm, D2 = D1+2

mm, and for the outer tube with the inner diameter D3 = D2+2 mm. Two alternative options, namely "warm He in the inner pipe" and "cold He in the inner pipe", were considered. In the preliminary calculations three possible correlations for the heat transfer coefficient were used and for the final calculations the most conservative one was chosen. It was shown that HEX made of copper tubes of length 5 m should ensure Tout < 15 K for the most demanding planned test conditions. HEX of length 6 m can also be made with steel tubes, however, in this case Tout max ≈ 18 K, it is close to its upper acceptable limit. It was also confirmed that for tests at low temperatures a bypass of the heat exchanger should be used, which requires installation of an additional "cold" valve in the cryogenic circuit. The option „warm He in the inner tube" seems more advantageous than the option "cold He in the inner tube", since it allows reduction of the pressure drop in the circuit.

Research on the effect of He+ irradiation [3] - to the dose of 7.5 dpa - with He ions of 0.25 and 2.0 MeV energy on the distribution of Cr atoms in three model (EFDA/EURATOM) $Fe_{100-x}Cr_x$ alloys (x=5.8, 10.75, 15.15) was a continuation of the one carried out in 2011-2012 in which the irradiation was done with 0.025 MeV He-ions. The measured distribution of Cr atoms in the irradiated samples was expressed in terms the Warren-Cowley short-range order (SRO) parameters: α_1 for the first-neighbour shell, α_2 for the second-neighbour shell, and α_{12} for the both shells. The obtained results (see exemplary Fig. 2) clearly demonstrate that short-range ordering depends both on Cr concentration and on energy of He ions.

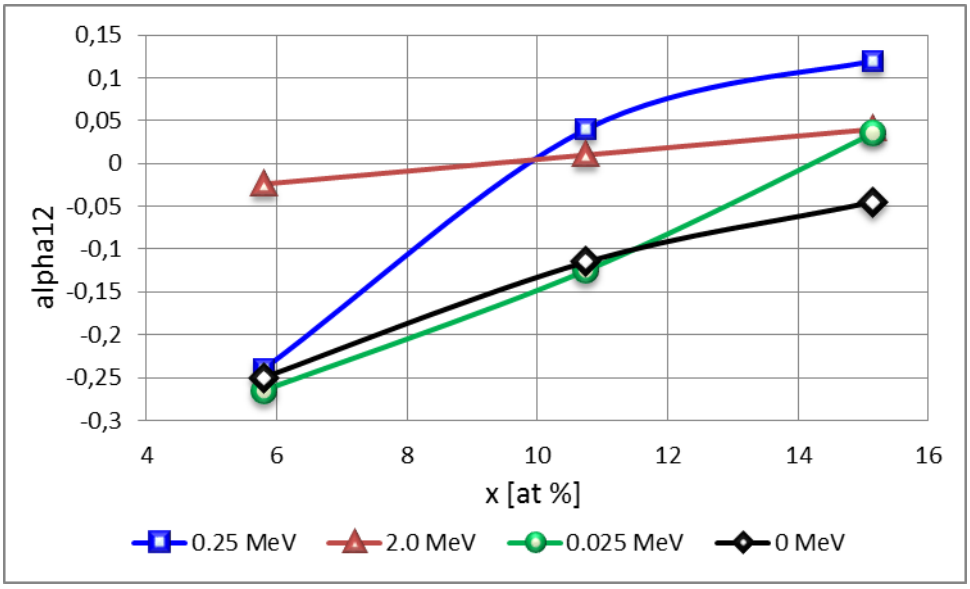

Fig. 2 Dependence of the SRO-parameter, α_{12}, on the concentration of chromium, *x*, in $Fe_{100-x}Cr_x$ alloys irradiated to the dose of 7.5 dpa with He-ions of various energy. Data for the non-irradiated and 0.025 MeV irradiated samples are also shown.

The effect of the following solution treatments [4]: T1 – annealing at 800K for 3 h in argon, followed by quenching into liquid nitrogen (80K), T2 – annealing at 800K for 3 h in argon, followed by quenching into water (290K) and T3 – annealing at 800K for 3 h in vacuum, followed by quenching onto a block of brass (295K) on short-range order in Fe-rich Fe-Cr alloys was also studied. The results obtained suggest that quenching into LN or H_2O (T1 and T2 treatments) resulted in a significant depletion of Cr atoms in the bulk of the samples as well as in a formation of Cr-substituted magnetite, hematite and wüstite on the samples' surface.

Fig. 3 shows the exemplary result of the study on the effect of plastic deformation on the kinetics of the σ-phase formation in an quasi-equiatomic Fe-Cr alloy [5]. The study, being a continuation of that from 2012, was aimed at investigation of the effect of a plastic deformation - between 60 and 97% - brought about by cold-rolling, on the kinetics of the sigma-phase formation in a quasi-equiatomic Fe-Cr alloy. The Mössbauer spectroscopy was used for that purpose.

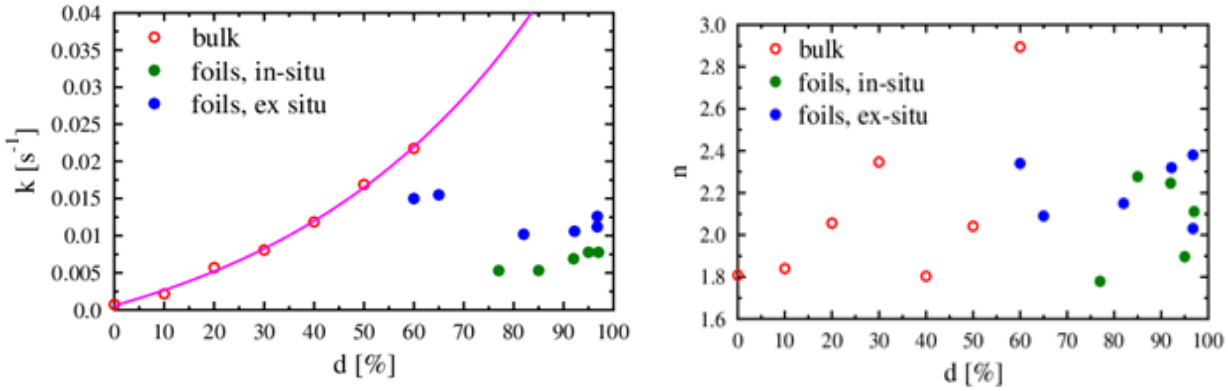

Fig. 3 (left) Dependence of the rate constant, *k*, on the degree of transformation, *d*, as found from the present *ex situ* (foils) measurements. (right) Dependence of the Avrami exponent, n, on the degree of transformation, d, as found from the present ex situ (foils) measurements.

Molecular Dynamics simulations [6] were conducted and analyzed in order to investigate helium bubble effect on mechanical properties of iron. Different bubble and matrix sizes were tested, along with changing bubble internal pressure. Impact of the helium presence inside the bubble was evaluated. All simulations were performed using LAMMPS software. The primary parameter measured during the simulation was von Mises stress, which allows to measure general impact of defects structure (in this case helium bubbles) on the mechanical properties of the material. Simulations have shown that the presence of the helium bubble significantly affects the mechanical properties of the material during shear deformation. An increase in the size of the bubble and the pressure exerted by the helium atoms on the walls of the matrix results in an increase of an average von Mises stress.

The influence of the TiC addition on the sinterability of W-TiC alloy has been studied [7]. Bimodal distribution of powder particles after MA was observed in the case of all W-TiC materials. Coarse particles were aggregated from smaller ~2 µm ones. All powders were contaminated with C, Fe and Cr elements caused by milling device made of stainless steel. The highest density was measured for material with 1.5%TiC, regardless the sintering method used. The specimens after cold compaction and sintering have microcracks. These microcracks were not observed in the PPS specimens. Significantly different microstructure with higher ~60% density was observed after PPS of the MA powder. Inhomogeneous microstructure of the W-TiC specimens with two kind of TiC particles, size ~250 nm and below 50 nm was observed.

The aim of this study devoted to silicon carbide to tungsten joints [8] was microstructural and phase composition examination of diffusion bonded SiC-W joints. Microstructure evaluation of polished tungsten surface was conducted by means of scanning electron microscopy (SEM). Energy and wavelength dispersive X-ray spectrometry for chemical composition measurement preceded phase composition analysis by X-ray diffraction (XRD). Additional evaluation of joint interface quality was performed with X-ray computed tomography (CT) and SEM on fracture surfaces of damaged samples. The study revealed that the quality of W/SiC joint interface was good. Concurrently high number of micro- and macroscopic defects in adjoining materials were observed which significantly deteriorated mechanical strength of the joint.

Conclusions

The ENEA design is characterized by larger helium cross sections as compared to the CRPP design. Despite that, the total helium mass flow rate in ENEA conductors is smaller than in the respective CRPP conductors, particularly in DL1. This is due to the fact that ENEA conductors have a large helium cross-section in the bundle regions, whereas the mass flow rate in the bundle regions is relatively small, due to the high hydraulic resistance. As a result the temperature margin for the removal of heat deposited by nuclear radiation in the DL1 in ENEA conductors is too small at 50 W heat deposition, whereas there is no temperature margin ($T_{out} > T_{cs}$) at the heat deposition of 100 W. Hence, we recommend to increase the diameter of the central cooling channel in the ENEA DL1 conductor.

Studying the preparation of the SULTAN facility for testing of high-current HTS conductors it was concluded that the heat exchanger of length 5 m made of copper tubes or of length 6 m made of steel tubes should fulfill all the assumed requirements.

Short-range ordering depends both on Cr concentration and on energy of He ions. The Cr-least concentrated alloy exhibits ordering of Cr atoms: its degree has been changed (diminished) only by the most energetic ions. The Cr-medium concentrated alloy shows a cross-over into clustering of Cr atoms in the samples irradiated with 0.25 and 2.0 MeV ions: the cross-over occurs at $x \approx 10$. The Cr-most concentrated alloy shows a cross-over into clustering of Cr atoms not only in the samples irradiated with 0.25 and 2.0 MeV ions but also with 0.025 MeV: for the latter the cross-over occurs at $x \approx 14$.

The results obtained in the study of the influence of heat reatment on iron alloys permit drawing the following conclusions: 1. SRO parameters in Fe-Cr are characteristic of a heat treatment. For a given treatment they are typical of a coordination shell (1NN, 2NN). 2. Quenching onto a block of brass resulted in a quasi-random distribution of Cr atoms within the 1NN-2NN volume for x<~15at%Cr, and clustering for higher x-values. The distribution in the individual coordination shells was, however, not random with an inversion at x≈5 going in the opposite direction. 3. Quenching into LN or H_2O resulted in a significant depletion of Cr atoms in the bulk of the samples as well as in a formation of Cr-substituted magnetite, hematite and wüstite on the samples' surface.

The study on the effect of plastic deformation on the kinetics of the σ-phase formation yields the following conclusions: (1) The kinetics of the σ-phase formation hardly depends on the deformation degree, d, for $d \geq 60\%$. (2) Avrami exponent (~2), hence the mechanism responsible for the transformation, does not meaningfully depend either on the deformation degree or on the transformation temperature. (3) The rate of the $\alpha \rightarrow \sigma$ phase transformation significantly depends on the annealing temperature, being the highest at 973K.

Four various W-TiC powder compositions were mechanically alloyed and consolidated using two sintering methods: classical powder metallurgy route (PM) and pulse plasma sintering (PPS). Density and microstructure of the obtained specimens were investigated. The results revealed that W-1.5%TiC material has the most promising properties.

W-SiC joints have been produced by diffusion bonding under nitrogen atmosphere. The quality of W/SiC interface was good, however high number of micro- and macroscopic defects in adjoining materials (cracks in SiC and voids in W) were observed which significantly deteriorated mechanical strength of the joined component.

Collaboration

Association EURATOM – ENEA, Frascati, Italy
Association EURATOM – CRPP PSI Villigen, Switzerland

References

[1] Final report on the Project "Iteration of the conductor analysis for both RW and WR options"
[2] Final report on the Project "Preparation of the SULTAN facility for testing of high-current HTS conductors at variable temperatures"
[3] Final report on the Project "Effect of He-ion irradiation on short-range ordering in model (EFDA) Fe-Cr alloys
[4] Final report on the Project "Effect of quenching medium on short-range order in Fe-rich Fe-Cr alloys"
[5] Final report on the Project "Effect of plastic deformation on the kinetics of the σ-phase formation in an quasi-equiatomic Fe-Cr alloy"
[6] Final report on the Project "Influence of helium bubble on mechanical properties of iron"
[7] Final report on the Project "Characterization of the W-TiC sintered material with various TiC contents"
[8] Final report on the Project "Development of joining technology for W-SiC structural joints"

3.5 Inertial fusion energy "keep-in-touch" activity

Corresponding author **Piotr Rączka**
piotr.raczka@ifpilm.pl

Introduction

The Inertial Fusion Energy "Keep-in-Touch" (IFE KiT) activity in 2013 involved the following tasks:

1. Analysis of emerging options of IFE on the basis of results of experiments and numerical modeling.
2. To inform the wider fusion community of developments in IFE.

The first task consisted of two sub-tasks: (a) a cooperative experiment on the phenomena relevant to shock ignition of ICF targets, performed by the IPPLM team at the PALS laboratory in Prague [1]; and (b) PIC simulations of laser-induced ion acceleration relevant for the ion fast ignition of ICF targets [2].

Activities relevant for the second task involved presentation of the results relevant to IFE at various general plasma and laser plasma conferences in Prague, Helsinki and Warsaw.

Results

According to the shock ignition concept in ICF the pellet containing DT fuel is first compressed by a laser pulse of moderate intensity (~10^{14} W/cm^2) and tens of ns duration, and just before stagnation it would be irradiated with a short (~ 0.2 – 0.5 ns) pulse of much higher intensity (~ 10^{16} W/cm^2), which should launch an igniting shock into the compressed fuel. One of the problems in this approach is the contribution of fast electrons to the ablation pressure on the target at supercritical density. In order to investigate this effect an experiment was performed on the PALS laser facility in Prague, in which a planar double-layered target consisting of a massive target made of Cu covered with a thin layer of CH was irradiated with two beams: a low intensity (~10^{14} W/cm^2) beam in the 1st harmonic (λ_1 = 1315 nm), which created a pre-plasma that simulated the plasma corona in ICF, followed by a high-intensity (~10^{15}-10^{16} W/cm^2) pulse in the 1st or 3rd harmonic (λ_3 = 438 nm) delayed by 1.2 ns relative to the auxiliary beam, which generated a shock that simulated the igniting shock. To determine the energy transfer from the laser beam to the target, the crater volume measurements were performed. To determine the electron density distribution the pre-plasma was diagnosed using the 3-frame interferometry. The measurements using these two diagnostics show that the presence of the pre-plasma strongly inhibits the fast electron contribution to the electron transfer in the case when the 1ω pulse is used to generate the shock, while the influence of pre-plasma was found insignificant in the case when the 3ω pulse is used to drive the shock [1].

The method of fast ignition of pre-compressed DT fuel pellets using a beam of laser-accelerated ions is a promising approach to Inertial Confinement Fusion, in which the process of fuel compression is disentangled form the process of ignition. The required ion beams could be conceivably generated by laser-driven acceleration provided that the laser-to-ion energy conversion efficiency is sufficiently high (i.e. above 10%), so that the energy of the igniting ps laser pulse does not exceed 100 kJ, which is considered to be a technological barrier. Particle-In-Cell simulations were performed for laser driven ion acceleration relevant for the ion fast ignition, to investigate the Laser Induced Cavity Pressure acceleration scheme, in which a target foil is placed in a cavity designed to redirect the reflected part of the laser pulse and thus recycle the laser energy that would be otherwise lost from the system. This scheme was devised to enhance the laser-to-ion energy conversion efficiency. The existing 1D PIC code was extended to multiple spatial dimension [2] and first results were obtained for LICPA acceleration in a model cavity at ultra-relativistic laser intensity of 2×10^{22} W/cm^2, where the dominant acceleration mechanism is that of photon pressure. Independently, a 1D PIC simulation of LICPA at moderately relativistic intensity of 10^{19} W/cm^2, when the acceleration of ions is due mainly to the sheath induced at the rear side of the target. In both cases a very encouraging increase in the laser-to-ion energy conversion efficiency was obtained relative to laser-driven acceleration in the conventional approach.

The IFE-relevant results obtained by the IPPLM team were communicated in talks presented at the Laser Energy Workshop, 2013 Optics & Optoelectronics SPIE Conference, Prague, 15-18 April, 2013, and posters presented at the 2013 EPS Conference on Plasma Physics, Helsinki, 1-5 July, 2013, and the conference Plasma 2013, Warsaw, 2-6 September 2013.

Conclusions

Concerning the shock ignition relevant experiment, the inhibiting influence of pre-plasma on energy transfer from the laser beam to the shock was found in the case of first harmonic. This suggests that fast electrons generated via resonance absorption may indeed contribute to the energy transfer.

Concerning the laser-driven ion acceleration for fast ignition, it was confirmed that the Laser Induced Cavity Pressure Acceleration scheme indeed ensures enhanced laser-to-ion energy conversion efficiency both at ultra-high laser intensities, through 2D simulations, and at moderately relativistic laser intensities, through 1D simulation.

Collaboration

Association EURATOM – IPP.CR, Prague, Czech Republic
P.N. Lebedev Phys. Inst. (FIAN), RAS, Moscow, Russia.
Central Laser Facility, Rutherford-Appleton Laboratory, Harwell Oxford, Didcot, UK.

References

[1] S.Yu. Gus'kov, N.N. Demchenko, A. Kasperczuk, T. Pisarczyk, Z. Kalinowska, T. Chodukowski, O. Renner, M. Smid, E. Krousky, M. Pfeifer, J. Skala, J. Ullschmied, and P. Pisarczyk, Laser-driven ablation through fast electrons in PALS experiment at the laser radiation intensity of 1-50 PW/cm^2, accepted for publication in Laser and Particle Beams.
[2] S. Jabłoński, Two-dimensional relativistic particle-in-cell code for simulation of laser-driven ion acceleration in various acceleration schemes, accepted for publication in Physica Scripta.